01 Oct 2010

Optimized Waveform Relaxation Solution of Electromagnetic and Circuit Problems

Martin J. Gander

Albert E. Ruehli
Missouri University of Science and Technology, ruehlia@mst.edu

Recommended Citation

M. J. Gander and A. E. Ruehli, "Optimized Waveform Relaxation Solution of Electromagnetic and Circuit Problems," *Proceedings of the 19th Topical Meeting on Electrical Performance of Electronic Packaging and Systems, 2010*, Institute of Electrical and Electronics Engineers (IEEE), Oct 2010.
The definitive version is available at https://doi.org/10.1109/EPEPS.2010.5642545

Optimized Waveform Relaxation Solution of Electromagnetic and Circuit Problems

Martin J. Gander* and Albert E. Ruehli+,
*Section of Mathematics, University of Geneva, Switzerland
+EMC Lab Missouri Univ. Science and Tech., Rolla, MO
Emeritus, IBM Research, Yorktown Heights, NY
albert.ruehli@gmail.com

***Abstract*— New algorithms are needed to solve electromagnetic problems using today's widely available parallel processors. In this paper, we show that applying the optimized waveform relaxation approach to a partial element equivalent circuit will yield a powerful technique for solving electromagnetic problems with the potential for a large number of parallel processor nodes.**

I. Introduction

In this paper, we introduce a method for the parallel solution of time domain combined ElectroMagetic (EM) and circuit problems. The EM part is represented with a Partial Element Equivalent Circuit (PEEC) model [1]. This transforms the EM part into an equivalent circuit model. The PEEC model is solved with the Modified Nodal Analysis (MNA) technique, that is also used in most Spice circuit solvers. Hence, this approach also leads to an EM solution which includes *dc* solutions important for chip and package applications.

The classical Waveform Relaxation (WR) approach was conceived in 1980/81 for circuit solver applications [2]. The approach is based on partitioning large circuits into many small circuits which then are solved separately on small Spice solvers. Sophisticated partitioning algorithms must be used for classical WR solvers as has been pointed out in [3]. The classical WR approach has a rich history of different techniques applied to a multitude of problems as summarized in [4]. In this paper, a new form of WR called optimized WR (oWR) is utilized. It is based on optimized *transmission* conditions which transfer the information between the subsystems. Basically, oWR is a subclass of domain decomposition techniques. The oWR approach was conceived for PDEs in [5], see also [6], [7]. It has been converted to the circuit domain, e.g., [8], [9].

Fundamentally, the approach divides the system matrix into as many subsystems (SSy) as are needed for the problem at hand. This permits the use of a large number of parallel processors. Further, the approach communicates waveforms in time between processors rather than transmitting the information at time points as is the case with other techniques. Also, the compute time for each SSy solution is not minute as is the case for some other algorithms, since we compute multiple time points or waveforms in time. Hence, the processor to processor communication latency is not as important for WR as it is for other algorithms. These aspects are of importance, for the efficient use of a large number of processors. Such algorithms are not easy to find as has been pointed out in [10]. Recent work for EM and circuit related works using the classical WR approach has yielded good results. The WR algorithm was applied to several electromagnetic problems, e.g., [11] where it was shown that the classical WR leads to a very efficient solution for the transverse partitioning of multiple transmission lines. As another example, the approach was applied to antenna arrays with a large number of elements [12].

The optimized WR approach is based on an improved transmission condition between SSys. In the classical WR, many different approaches have been experimented with for the transmission condition for the circuit information exchange between SSys. Techniques, related to non-optimized circuits and overlap type partitioning for circuits, are referenced in the overview paper [4] and also in [13]. We will show that optimization is key for the performance gain. Overlapping circuits are related to overlapping domains in domain decomposition methods [7]. The new transmission conditions use a combination of multiple optimized variables such that the convergence is sped up. Importantly, we have shown that circuits which failed to converge with classical WR converge relatively fast with oWR. A key problem is the choice of the optimization parameters. They are easier to deterimine for the known topology of a PEEC circuit. Our studies in earlier work have helped us to understand the choice of the parameters. Fortunately, the fast convergence issue is not sensitive to the choice of the optimization parameters. In earlier work we viewed the parameters in terms of formulas. Importantly, in this paper, we present a circuit interpretation for the transmission conditions which considerably simplifies the oWR concepts, and it enhances the understanding of the approach.

II. Small model circuit

We consider only a two fundamental section PEEC circuit shown in Fig. 1 for the analytical model since it contains the situation we need to address. In this work, we use consistent normalized units for all experiments which are mA, V, kOhm, pF, μH, GHz and ns. We set up the usual MNA circuit equations to determine the best oWR model. The details for

978-1-4244-6867-6/10/$26.00 ©2010 IEEE

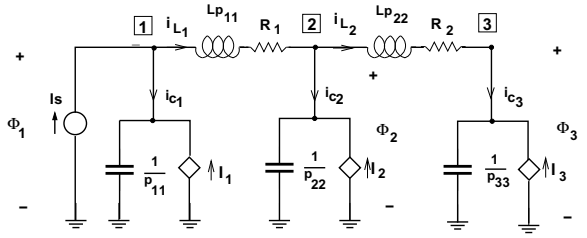

Fig. 1. PEEC circuit model with two basic sections

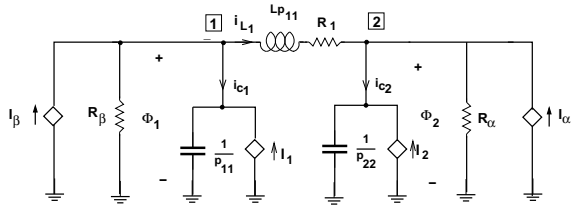

Fig. 2. PEEC circuit with models which includes transmission condition

the PEEC model are given in [14]. The delay equations for the capacitance are given by

$$\begin{aligned} I_1 &= \frac{p_{12}}{p_{11}} ic_2(t-\tau_{12}) + \frac{p_{13}}{p_{11}} ic_3(t-\tau_{13}), \\ I_2 &= \frac{p_{21}}{p_{22}} ic_1(t-\tau_{12}) + \frac{p_{23}}{p_{22}} ic_3(t-\tau_{23}), \\ I_3 &= \frac{p_{31}}{p_{33}} ic_1(t-\tau_{13}) + \frac{p_{32}}{p_{33}} ic_2(t-\tau_{23}). \end{aligned} \tag{1}$$

At node 1, we get the KCL equations

$$i_{c1} = -i_{L1} + I_s, \tag{2}$$

and for the intermediate node 2, solved for the capacitance current

$$i_{c2} = i_{L1} - i_{L2}. \tag{3}$$

Finally, the capacitive current for node 3 is simply

$$i_{c3} = i_{L2}. \tag{4}$$

Inserting (2) and (3) into (1), we obtain

$$\begin{aligned} I_1 &= \frac{p_{12}}{p_{11}} \left[i_{L1}(t-\tau_{12}) - i_{L2}(t-\tau_{12}) \right] + \frac{p_{13}}{p_{11}} i_{L2}(t-\tau_{13}), \\ I_2 &= \frac{p_{21}}{p_{22}} \left[-i_{L1}(t-\tau_{12}) + I_s(t-\tau_{12}) \right] + \frac{p_{23}}{p_{22}} i_{L2}(t-\tau_{23}), \\ I_3 &= \frac{p_{31}}{p_{33}} \left[-i_{L1}(t-\tau_{13}) + I_s(t-\tau_{13}) \right] + \frac{p_{32}}{p_{33}} \left[i_{L1}(t-\tau_{23}) - i_{L2}(t-\tau_{23}) \right]. \end{aligned}$$

For the impedance part of the MNA equations, we have

$$\begin{aligned} -\Phi_1 + Lp_{11} \frac{di_{L1}}{dt} + Lp_{12} \frac{di_{L2}(t-\tau_L)}{dt} + R_1 i_{L1} + \Phi_2 &= 0, \\ -\Phi_2 + Lp_{22} \frac{di_{L2}}{dt} + Lp_{21} \frac{di_{L1}(t-\tau_L)}{dt} + R_2 i_{L1} + \Phi_3 &= 0. \end{aligned} \tag{5}$$

Corresponding to the above formulation, the frequency domain MNA circuit matrix M for this case is given by

$$\begin{bmatrix} \frac{s}{p_{11}} & 1 - \frac{p_{12}}{p_{11}} e^{-s\tau_{12}} & 0 & \frac{p_{12}}{p_{11}} e^{-s\tau_{12}} - \frac{p_{13}}{p_{11}} e^{-s\tau_{13}} & 0 \\ 1 & -sLp_{11} - R_1 & -1 & -sLp_{12} e^{-s\tau_L} & 0 \\ 0 & -1 + \frac{p_{21}}{p_{22}} e^{-s\tau_{12}} & \frac{s}{p_{22}} & 1 - \frac{p_{23}}{p_{22}} e^{-s\tau_{23}} & 0 \\ 0 & -sLp_{21} e^{-s\tau_L} & 1 & -sLp_{22} - R_2 & -1 \\ 0 & \frac{p_{31}}{p_{33}} e^{-s\tau_{13}} - \frac{p_{32}}{p_{33}} e^{-s\tau_{23}} & 0 & -1 + \frac{p_{32}}{p_{33}} e^{-s\tau_{23}} & \frac{s}{p_{33}} \end{bmatrix} \tag{6}$$

and the corresponding system is

$$\boldsymbol{M}\boldsymbol{x} = \boldsymbol{b}, \tag{7}$$

with

$$\boldsymbol{x} = \begin{bmatrix} \Phi_1 & i_{L1} & \Phi_2 & i_{L2} & \Phi_3 \end{bmatrix}^T \tag{8}$$

and

$$\boldsymbol{b} = \begin{bmatrix} I_s & 0 & \frac{p_{21}}{p_{22}} I_s e^{-s\tau_{21}} & 0 & \frac{p_{31}}{p_{33}} I_s e^{-s\tau_{13}} \end{bmatrix}^T. \tag{9}$$

Hence, the solution for the model in Fig. 1 in the frequency domain is defined by the system (7).

III. Transmission conditions for WR

The partitioning step for the *WR* approach consists of breaking connections between multiple SSys such that the SSys are independent. In our example of the PEEC circuit here, we obtain the MNA sub-circuit matrices by partitioning (6) with the dublication of node 2 as

$$M_1 := \begin{bmatrix} \frac{s}{p_{11}} & 1 - \frac{p_{12}}{p_{11}} e^{-s\tau_{12}} & 0 \\ 1 & -sLp_{11} - R_1 & -1 \\ 0 & -1 + \frac{p_{21}}{p_{22}} e^{-s\tau_{12}} & \frac{s}{p_{22}} \end{bmatrix} \tag{10}$$

and

$$M_2 := \begin{bmatrix} \frac{s}{p_{22}} & 1 - \frac{p_{23}}{p_{22}} e^{-s\tau_{23}} & 0 \\ 1 & -sLp_{22} - R_2 & -1 \\ 0 & -1 + \frac{p_{32}}{p_{33}} e^{-s\tau_{23}} & \frac{s}{p_{33}} \end{bmatrix}, \tag{11}$$

and the coupling vectors between SSy1 and SSy2 are given by

$$\boldsymbol{m}_1 := \begin{bmatrix} \frac{p_{12}}{p_{11}} e^{-s\tau_{12}} - \frac{p_{13}}{p_{11}} e^{-s\tau_{13}} \\ -sLp_{12} e^{-s\tau_L} \\ 1 - \frac{p_{23}}{p_{22}} e^{-s\tau_{23}} \end{bmatrix}, \tag{12}$$

and

$$\boldsymbol{m}_2 := \begin{bmatrix} -1 + \frac{p_{21}}{p_{22}} e^{-s\tau_{12}} \\ -sLp_{21} e^{-s\tau_L} \\ \frac{p_{31}}{p_{33}} e^{-s\tau_{13}} - \frac{p_{32}}{p_{33}} e^{-s\tau_{23}} \end{bmatrix}. \tag{13}$$

One classical partitioned WR solution for the first SSy is to set i_{L2} to zero until updated unknowns are available from the WR iterations. Denoting the unknowns of the first sub-circuit by $\boldsymbol{x}(s_1) := (\Phi_1(s_1), i_{L1}(s_1), \Phi_2(s_1))^T$, and the unknowns of the second subsystem by $\boldsymbol{x}(s_2) := (\Phi_2(s_2), i_{L2}(s_2), \Phi_3(s_2))^T$, and similarly for $\boldsymbol{b}$, we obtain the classical WR algorithm

$$M_1 \boldsymbol{x}^k(s_1) = \boldsymbol{b}(s_1) - \boldsymbol{m}_1 i_{L2}^{k-1}(s_1), \tag{14}$$

$$M_2 \boldsymbol{x}^{k+1}(s_2) = \boldsymbol{b}(s_2) - \boldsymbol{m}_2 i_{L1}^{k}(s_2), \tag{15}$$

where k is the WR iteration index. The unknown currents $i_{L2}^k(s_1)$ and $i_{L1}^k(s_2)$ on the right are relaxed to the previous iteration, by imposing the transmission conditions

$$\begin{aligned} i_{L2}^k(s_1) &= i_{L2}^{k-1}(s_2), \\ i_{L1}^{k+1}(s_2) &= i_{L1}^k(s_1). \end{aligned} \tag{16}$$

For space reasons, in Fig. 2 we give an equivalent circuit for an SSy where each side has the additional oWR circuit elements. For the classical case, only current or voltage is transmitted across the interface. The added resistors inside of the SSY are key for the oWR approach. In the oWR, we are exchanging more than one variable for which the weight is optimized. For the problem at hand, we subdivide the system

into the same two SSys as before, but for reasons which will be apparent below, we now use the following transmission condition between SSy1 (s1) and SSy2 (s2):

$$i_{L2}^{k}(s_1) + G_\alpha \Phi_2^k(s_1) = i_{L2}^{k-1}(s_2) + G_\alpha \Phi_2^{k-1}(s_2), \quad (17)$$

$$i_{L1}^{k+1}(s_2) + G_\beta \Phi_2^k(s_2) = i_{L1}^{k}(s_1) + G_\beta \Phi_2^k(s_1). \quad (18)$$

The parameters, or conductances which are optimized in the oWR circuit are G_α for one direction and G_β for the coupling in the other direction. It is obvious from the equations why we label the adjustable parameters as conductances.

IV. Improved convergence for oWR circuit

In this section we illustrate the improved convergence of the oWR algorithm. The conductances G_α and G_β are adjustable circuit elements which we can choose such that the algorithm converges more rapidly. We illustrate this for the model circuit in Fig. 1. We use the circuit element values from [14] as

$$Lp_{11} = 0.022362,\ Lp_{12} = 0.006314,$$
$$Lp_{21} = 0.006314,\ Lp_{22} = 0.022362;$$

$$p_{11} = 1.19143,\ p_{12} = 0.300756,\ p_{21} = 0.300756,$$
$$p_{22} = 0.80392,\ p_{33} = 1.19143,\ p_{13} = 0.121378,$$
$$p_{31} = 0.121378,\ p_{23} = 0.300756,\ p_{32} = 0.300756;$$

$$R_1 = 0.001,\ R_2 = 0.001;$$

$$t_{12} = 0.167,\ t_{13} = 0.333,\ t_{23} = 0.167,\ t_L = 0.167.$$

Using substantial analysis which is beyond the scope of this short paper, we can compute contraction factors $\rho(\omega)$ for both the classical WR and the oWR at each frequency $s = j\omega$. This represents the number by which the error is multiplied by WR or oWR at a given frequency for each iteration. One can show that $\rho(\omega) = \rho(-\omega)$, and it is sufficient to consider positive frequencies. However, the direct connection between neighboring SSy also leads to low frequency coupling. However, we show that for oWR the contraction is substantially improved. This is evident from Figs. 6 and 7 in the example, where the optimized parameters in Fig. 6 lead to a faster low frequency, large time convergence. Also, the transient solution is computed for a bounded solution time interval $(0, T)$, in our example $T = 5$. This contains the low frequency spectrum, to $\omega_{\min} > 0$. In Fig. 3, we compare the contraction factor for the classical and the oWR. For the circuit parameter given, the best conductances were found to be $G_\alpha = -1.2412$ and $G_\beta = 8.1169$. One can clearly see that classical WR is not convergent for the critical angular frequencies ω around ± 10 since the contraction factor is larger than one. Hence the method would diverge if sufficient energy excites these frequencies. This is different for oWR, which has a substantially improved contraction factor. It is now uniformly less than one, which means all frequencies ω are convergent. We see that the optimal choice of G_α and G_β leads to equioscillation of the convergence factor: it is the same for the lowest and the difficult frequency around $\omega = 10$. We note that on a bounded time interval even classical WR will converge eventually, since WR algorithms converge ultimately superlinearly, and even modes that have a contraction factor larger than one in our analysis will eventually converge. Next, we give a numerical experiment to illustrate that this convergence is slow.

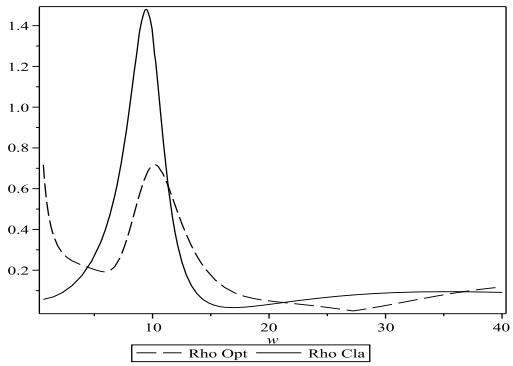

Fig. 3. Comparison of the contraction factor of the classical WR and the oWR algorithm, for each angular frequency ω

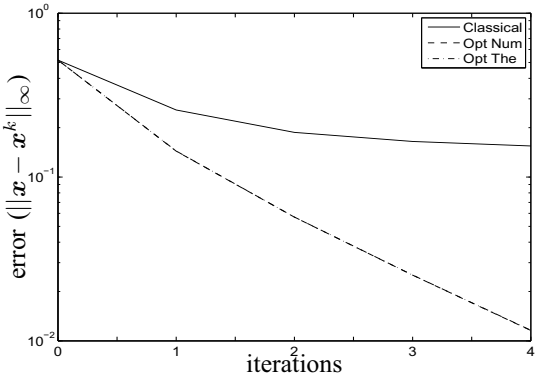

Fig. 4. Convergence behavior of the classical (top curve) and optimized WR algorithm for the theoretically optimized G_α and G_β and their numerically optimized counterparts, which are very close (bottom curves)

We discretize the MNA equations for the model circuit in Fig. 1 using a backward Euler integration with time step $\Delta t = 1/768$, and use as the input current I_s a linear triangle function, which grows for $0 < t < 0.05$ to 1, and then decreases for $0.05 < t < 0.1$ back to zero, where it remains for $t > 0.1$. The circuit is solved on the time interval $(0, T)$ for $T = 5$. We show in Fig. 4 the convergence behavior of the classical algorithm compared to the theoretically optimized one with $G_\alpha = -1.2412$ and $G_\beta = 8.1169$. The best possible choice of the optimization conductances also was also by using numerical optimization to minimize the error ($||x - x^k||_\infty$) after 4 iterations. It led to $G_\alpha = -1.1723$ and $G_\beta = 8.359$. This confirms that both the theoretical and the experimental optimized admittance parameters are very close.

V. Numerical example results

We choose the two conductor problem in Fig. 5 to illustrate the practical partitioning of a strong *dc* coupled path. It is important to include the full wave retardation between the elements for the relatively fast rise time of the applied signal. The structure, which is 50 mm long, is excited with a linear ramp current source which has a 200 ps rise time. The

Fig. 5. Example PEEC problem with two wires

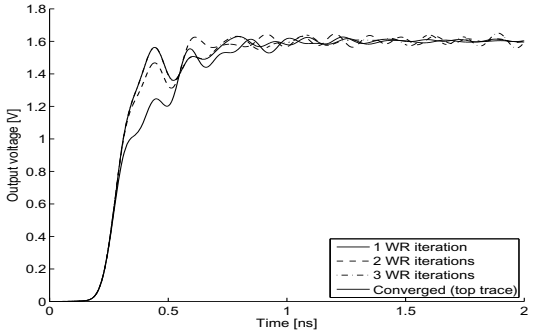

Fig. 6. Convergence with good convergence conductances

magnitude of the current is 10 mA. We represent each wire with 10 PEEC cells as shown in Fig. 5, which is relatively few. The flat wires are 2 mm wide and are spaced 5mm and the two wires are connected with a termination resistance of $R_T = 0.2$ kOhms. For the experiments, we subdivide the structure into two parts, where each of the parts has 5 sections. All the far coupled partial inductances and capacitive current sources are taken into account by using classical WR as it was done in [12], where it was shown that the far coefficient WR convergence is extremely fast and that we can determine approximate convergence conditions. In Fig. 6 we show that oWR converges to the solution in very few iterations. For this case, the optimized conductances are $G_\alpha = -1.9$ and $G_\beta = 2.4$. As a sensitivity experiment, we increased both values 5 times and the results in Fig. 7 to show that, while the convergence is less uniform, it is still quite fast. In Fig. 8, we show that for the case where $G_\alpha = 0$ and $G_\beta = 2.4$, the convergence is very slow, as expected. This illustrates the effectiveness of the oWR approach presented in this paper.

VI. Conclusions

The oWR method given in this paper represents a major improvement in the convergence rate for waveform relaxation. A new circuit interpretation is given for the transmission conditions. It is also shown that the WR approach can successfully

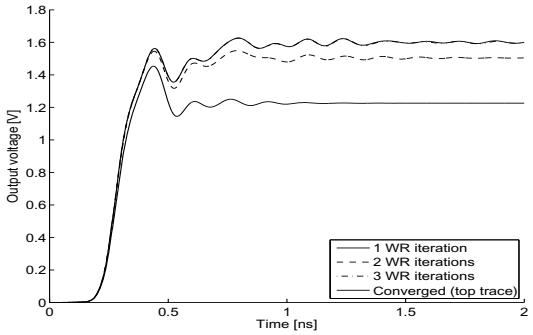

Fig. 7. Convergence with five times larger convergence conductances

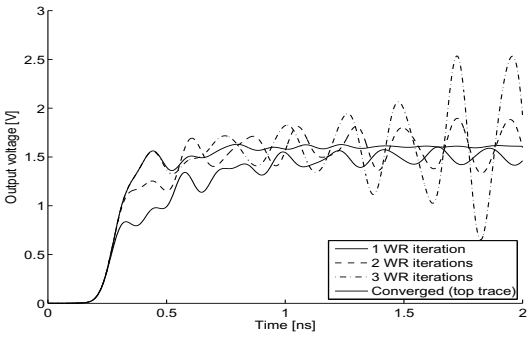

Fig. 8. Convergence test with forward optimization turned off

be applied to delayed full wave PEEC models. Further, the models which before had converged very slowly can converge in very few iterations. This is an important step forward since this approach is key for partitioned multiprocessor solution methods.

References

[1] A. E. Ruehli, G. Antonini, J. Esch, J. Ekman, A. Mayo and A. Orlandi. Non-orthogonal PEEC formulation for time and frequency domain EM and circuit modeling. *IEEE Transactions on Electromagnetic Compatibility*, 45(2):167–176, May 2003.

[2] E. Lelarasmee, A. E. Ruehli, and A. L. Sangiovanni-Vincentelli. The waveform relaxation method for time-domain anaylsis of large-scale integrated circuits. *IEEE Trans. on CAD of Integrated Circuits and Systems*, CAD-1(3):131–145, July 1982.

[3] H. Peng and C.-K. Cheng. Parallel transistor level fulll-chip circuit simulation. In *Design Automation and Test in Europe*, pages 304–307, Nice, France, April 2009.

[4] A. E. Ruehli and T. A. Johnson. *Circuit Analysis Computing by waveform relaxation*, volume 3. Wiley Encyclopedia of Electrical Electronics Engineering, New York, 1999.

[5] M. J. Gander, L. Halpern, and F. Nataf. Optimal convergence for overlapping and non-overlapping Schwarz waveform relaxation. In C-H. Lai, P. Bjørstad, M. Cross, and O. Widlund, editors, *Eleventh international Conference of Domain Decomposition Methods*. ddm.org, 1999.

[6] M. J. Gander, L. Halpern, and F. Nataf. Optimal Schwarz waveform relaxation for the one dimensional wave equation. *SIAM Journal of Numerical Analysis*, 41(5):1643–1681, 2003.

[7] M. J. Gander and L. Halpern. Optimized Schwarz waveform relaxation methods for advection reaction diffusion problems. *SIAM J. Numer. Anal.*, 45(2):666–697, 2007.

[8] M. J. Gander and A. Ruehli. Optimized waveform relaxation methods for RC type circuits. *IEEE Transactions on Circuits and Systems*, 51(4):755–768, 2004.

[9] M. J. Gander M. Al-Khaleel and A. E. Ruehli. Optimized waveform relaxation methods for logitudinal partitioing of transmission lines. *IEEE Transactions on Circuits and Systems I*, 56(8):1732–1773, 2009.

[10] D. Patterson. The trouble with multi-core microprocessors. *IEEE Spectrum Magazine*, 47(3):28, July 2010.

[11] N. J. Nakhla, A. E. Ruehli, M. S. Nakhla, R. Achar and C. Chen. Waveform relaxation techniques for simulation of coupled interconnects with frequency-dependent parameters. *IEEE Transactions on Advanced Packaging*, 30(2):257–269, 2007.

[12] G. Antonini and A. E. Ruehli. Waveform relaxation time domain solver for subsytem arrays. *IEEE Transactions on Advanced Packaging*, accepted for publication 2010.

[13] V.B. Dmitriev-Zdorov and B. Klaassen. An improved relaxation approach for mixed system analysis with several simulation tools. In *EURO-DAC '95/EURO-VHDL '95*, pages 274–279. IEEE Computer Society Press, 1995.

[14] A. E. Ruehli, U. Miekkala, and H. Heeb. Stability of discretized partial element equivalent EFIE circuit models. *IEEE Transactions on Antennas and Propagation*, 43(6):553–559, June 1995.